Towards assessing CO_2 emissions from fossil fuel combustion by GOSAT observations of localized CO_2 enhancements

Rajesh Janardanan[1], Shamil Maksyutov[1], Tomohiro Oda[2], Makoto Saito[1], Johannes W. Kaiser[3], Alexander Ganshin[4], Andreas Stohl[5], Tsuneo Matsunaga[6], Yukio Yoshida[1] and Tatsuya Yokota[1]

[1]CGER, NIES, Japan; [2]GSFC/USRA, USA; [3]MPIC, Germany; [4]CAO/TSU, Russia; [5]NILU, Norway; [6]CEMA, NIES, Japan

Email: rajesh.janardanan@nies.go.jp

Introduction

- Emissions from fossil fuel use is the major sources of atmospheric carbon dioxide.
- Megacities and power plants contribute a large proportion of these emissions.
- We demonstrate the capability of Greenhouse gas Observing SATellite (GOSAT) to detect local enhancements caused by emissions from fossil fuel use.
- We made an attempt to deduce fossil fuel emission signal of CO_2 in GOSAT observed total column dry air mole fractions of CO_2 (X_{CO2}) for a period June 2009 through December 2012.

Data

- **The meteorological data** JCDAS (1.25°×1.25°) and 40 vertical hybrid sigma-pressure levels. The temporal resolution of input data is 6 h.
- **Satellite XCO_2 data** NIES GOSAT SWIR X_{CO2} Level 2 product (V2.11)
- **Fossil fuel emission** Open source Data Inventory of Anthropogenic CO_2 emission (ODIAC) inventory, a global 0.1°×0.1°.
- **Fire emission inventory** Global Fire Assimilation Syatem (GFASv1.0) (Kaiser et al., 2011)
- **Biospheric fluxes** from Vegetation Integrative Simulator of Trace gases (VISIT) at 0.1°

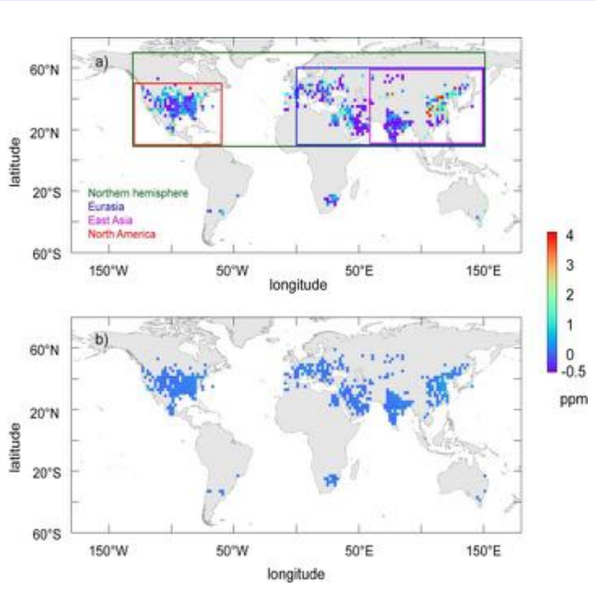

Figure 1. Observed and simulated total column CO_2 with significant fossil fuel signature averaged over 2°×2° grid. a) GOSAT-deduced fossil fuel enhancements in X_{CO2} ($\Delta X_{CO2,obs}$; colour shading; ppm) averaged over 2°×2° grid where atleast 10 observations exist for 2009–2012. The macro regions—East Asia (10–60°N, 60–150°E), Eurasia (10–60°N, 0–150°E), North America (10–50°N, 130–60°W) and the Northern Hemisphere (10–70°N, 130°W–150°E)—used for regional regression between modelled and observed ΔX_{CO2} are shown by coloured rectangles. Overlapping boundaries are drawn with 1° offset for visual clarity. **b)** Simulated fossil fuel enhancements in X_{CO2} ($\Delta X_{CO2,sim}$; colour shading; ppm)

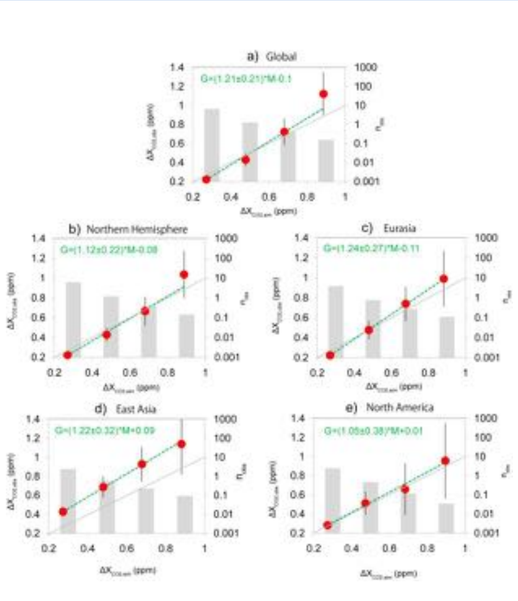

Figure 2. Mean observed ($\Delta X_{CO2,obs}$) versus simulated ($\Delta X_{CO2,sim}$) enhancements in **0.2 ppm bins for a)** Globe, **b)** Northern Hemisphere, **c)** Eurasia **d)** East Asia and **e)** North America. Vertical thin lines show the standard error of the mean observed enhancements. Standard errors in the binning of simulated values are smaller than the symbol size. The grey dashed line is the "identity line". The error-weighted regression between the modelled and observed X_{CO2} enhancements is shown as the green dashed line. The regression equation is shown at the top left of each panel (G, GOSAT; M, Model). The grey bars give the number of observations in thousands (right vertical axis, logarithmic scale; read n_{obs} as $n_{obs}\times10^3$) in each enhancement bin.

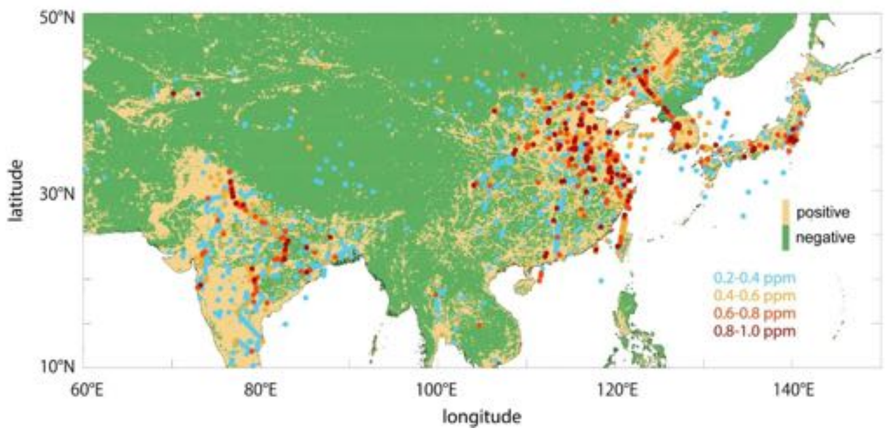

Figure 3. Simulated enhancements for East Asian domain and comparison between ODIAC and EDGAR. Observation locations (coloured dots) corresponding to 0.2-1 ppm X_{CO2} abundance ($\Delta X_{CO2,sim}$) over East Asian domain. The colour shading over the map shows the difference between ODIAC and EDGAR inventories for the years 2008–2010 (yellow-ODIAC higher, green-ODIAC lower).

Methods

Lagrangian transport simulation

- for all GOSAT scans for a period from June 2009 until December 2012 using the Lagrangian Particle Dispersion model (LPDM) FLEXPART with fossil fuel, biomass burning and biospheric CO_2 fluxes, each calculates $\Delta X_{CO2,ff}$, $\Delta X_{CO2,fire}$, $\Delta X_{CO2,veg}$ at resolution (0.1°) comparable to GOSAT observation footprint (figure 6).

ΔX_{CO2} from GOSAT

- We used GOSAT observations on locations where simulated enhancements due to emissions from fossil fuel ($\Delta X_{CO2,ff}$) exceed 0.1 ppm for estimating the enhancement over mean of clean surrounding observations.
- Remove the influence of biospheric and biomass burning emissions from the observed X_{CO2} by subtracting the model simulated concentration with respective fluxes. We calculate the mean of observations (X_{CO2}) for locations corresponding to $\Delta X_{CO2,ff}$ <0.1ppm (which are considered as clean pixels in simulation) for each monthly subsets in 10°×10° rectangular regions where the number of these clean pixels are greater than 16.
- These are designated as background mixing ratios ($X_{CO2,bg}$) that are relatively free from fossil fuel emissions. $\Delta X_{CO2,obs}$ is then calculated as

$$\Delta X_{CO2,obs} = X_{CO2,obs} - X_{CO2,bg}$$

- These values were categorized in to 0.2 ppm bins based on model simulations. These values were aggregated for the whole period of study and subjected to linear regression with the model calculated values.

$$\Delta X_{CO2,ff} = \Delta X_{CO2,obs} - \Delta X_{CO2,veg} - \Delta X_{CO2,fire}$$

- The regression was carried out for regions mentioned in Fig. 1a with weight to the standard error in mean observed enhancements in each bin.

Results

- The X_{CO2} abundance corresponding to emissions from fossil fuel over global and regional domains calculated by FLEXPART ($\Delta X_{CO2,ff}$) and those estimated from GOSAT observation ($\Delta X_{CO2,obs}$) show linear relations in each 0.2 ppm enhancement bins below 1.0 ppm (Fig. 2).
- Over East Asia, the regression analysis gave a higher slope value (1.22±0.32; Fig. 2d), and an offset (fig. 5) from indicating that on average, the simulated enhancements ($\Delta X_{CO2,ff}$) are lower than the observed ones.
- The slope value and proximity to one-to-one line over different regions results from the simulated enhancements and which in turn depends mainly on the CO_2 emission inventory used in the model.
- The discrepancy between simulated and observed X_{CO2} abundance (22%) and its uncertainty (32%) over East Asia are comparable to the uncertainties (~15%) associated with fossil fuel CO_2 emission over this region (eg. *Zhao et al.*, 2012).
- A study (*Zhao et al.*, 2012) recompiling the Chinese CO_2 emissions using provincial level energy statistics revealed that CO_2 emission from fossil fuel and cement production showed notable differences with generally accepted estimates (eg. 5-10% higher than CDIAC during 2005-2009). These uncertainties in the national total CO_2 emissions are potentially propagated to derived global emission data sets and our model simulations.
- observations corresponding to simulated enhancements in the range of 0.2 to 1 ppm in East Asia are largely clustered over eastern China and India where fossil fuel emissions and the uncertainties in them are high (figure 3).
- The number of observations having strong fossil fuel signal is small (figure 7), thus limiting the analysis to below 1ppm owing to the growing uncertainty (figure 4)
- With the precision and number of GOSAT observations, it is possible to monitor emissions from strong CO_2 sources such as power plants and megacities for regions with elevated CO_2 column abundance in the range of 0.2 to 1 ppm.
- This method will be useful in monitoring fossil fuel emissions, especially in the context of recent reports on disparities in fossil fuel use and CO_2 emission in China (*Guan et al,* 2012).

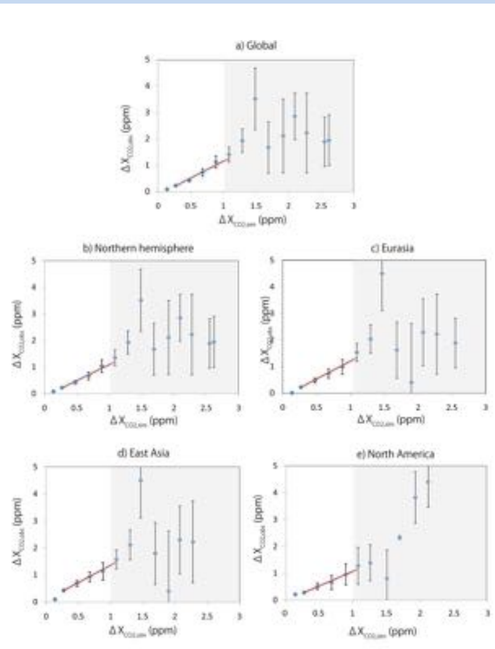

Figure 4. Mean observed ($\Delta X_{CO2,obs}$) versus simulated ($\Delta X_{CO2,sim}$) enhancements in 0.2 ppm bins for a) Globe, b) Northern Hemisphere, c) Eurasia d) East Asia and e) North America. Vertical thin lines show the standard error of the mean observed enhancements. The error-weighted regression between the modelled and observed X_{CO2} enhancements is shown as the red line. The grey shaded region demarcate the observations (beyond 1 ppm) which were not used in regression due to the apparently large noise in the data.

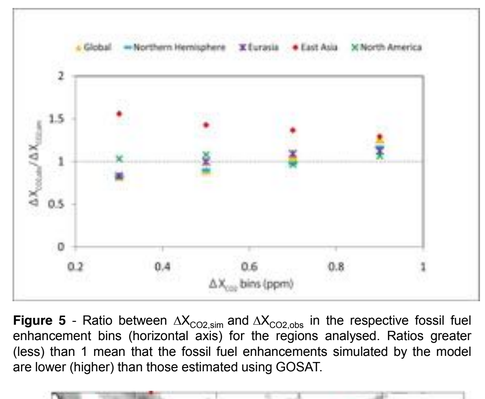

Figure 5 - Ratio between $\Delta X_{CO2,sim}$ and $\Delta X_{CO2,obs}$ in the respective fossil fuel enhancement bins (horizontal axis) for the regions analysed. Ratios greater (less) than 1 mean that the fossil fuel enhancements simulated by the model are lower (higher) than those estimated using GOSAT.

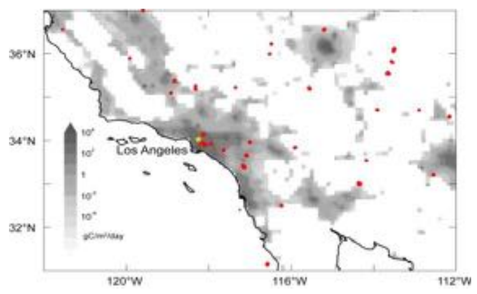

Figure 6. GOSAT observation footprints for Los Angeles (yellow mark) megacity region. The grey shading is the CO_2 emission (gC/m²/day). Red dots are GOSAT observations (size approximately in scale to GOSAT surface footprints) selected according to simulated fossil XCO_2 greater than 0.1 ppm.

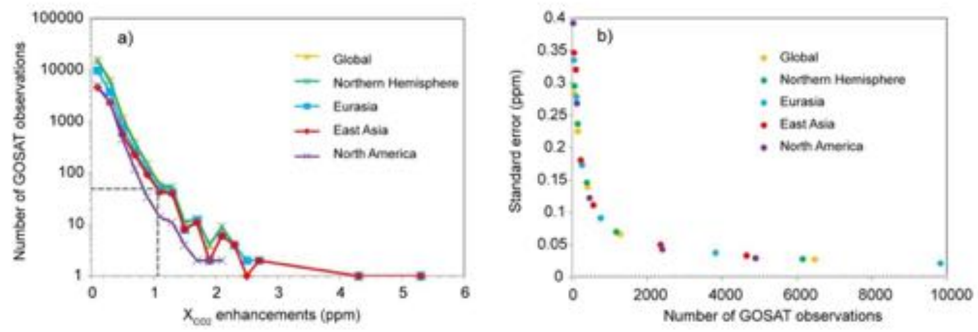

Figure 7. a) Number of available GOSAT observations in each 0.2 ppm bins for all the regions of analysis. The number of observations are less than 50 for X_{CO2} abundance greater than 1 ppm (marked by grey dashed lines). b) Standard error in bin averaged enhancements ($\Delta X_{CO2,obs}$) versus number of observation in the respective fossil fuel enhancement bins for the regions analysed. We have omitted bins with less than 50 observations. Since the data count varies for different regions, we have used up to 1 ppm enhancements for regression analysis for uniformity.

Summary

- Observed and simulated XCO_2 enhancements around large sources due to emissions from fossil fuel use is analyzed for different regions.
- These observed and simulated XCO_2 abundance agree well for larger regions, but show differences over East Asia.
- Such independent monitoring of emission from space could be useful to detect potential biases in reported emissions.
- Our results suggest that considerably better performance can be expected for emission monitoring from OCO-2 and future missions which can see larger enhancements in same plumes with a smaller footprint and can produce more observations than GOSAT.

Reference

- Yokota, T., Yoshida, Y., Eguchi, N., Ota, Y., Tanaka, T., Watanabe, H. & Maksyutov, S. Global Concentrations of CO_2 and CH_4 Retrieved from GOSAT: First Preliminary Results, ***SOLA***, 5,160-163, (2009)
- Oda, T. & Maksyutov, S. A very high-resolution (1 km×1 km) global fossil fuel CO_2 emission inventory derived using a point source database and satellite observations of nighttime lights. ***Atmos. Chem. Phys***. 11, 543-556 (2011)
- Saito, M., Maksyutov, S., Hirata, R., and Richardson, A. D. An empirical model simulating diurnal and seasonal CO2 flux for diverse vegetation types and climate conditions, **Biogeosciences**, 6, 585–599, doi: 10.5194/bg-6-585-2009, 2009
- Kaiser, J.W., Heil, A., Andreae, M.O., Benedetti, A., Chubarova, N., Jones, L., Morcrette, J.J., Razinger, M., Schultz, M. G., Suttie, M., and van der Werf, G. R. Biomass burning emissions estimated with a global fire assimilation system based on observed fire radiative power, **Biogeosciences**, 9, 527–554, 2012
- Guan, D. B., Liu, Z., Geng, Y., Lindner, S. and Hubacek, K. (2012) The gigatonne gap in China's carbon dioxide inventories. ***Nature Clim. Change*** 2, 672–675, doi:10.1038/nclimate1560.
- Zhao, Y., Nielsen C. P., and McElroy M. B. (2012) China's CO_2 emissions estimated from the bottom up: Recent trends, spatial distributions, and quantification of uncertainties, ***Atmos. Env***. 59, 214–223.